

New Thermal Ink Jet Printhead with Improved Energy Efficiency Using Silicon Reactive Ion Etching

Masahiko Fujii,[▲] Toshinobu Hamazaki* and Kenji Ikeda

New Marking Development Department, Fuji Xerox Co., Ltd., Kanagawa-pref., Japan

*Marking Device Development Department, Fuji Xerox Co., Ltd., Kanagawa-pref., Japan

In thermal ink jet (TIJ) printhead design, in order to satisfy various market demands, it is important to consider how effectively the printhead transfers input energy to ejected drop performance. First, we defined energy efficiency as a ratio of ejected ink drop energy (the sum of kinetic and surface energy) to consuming electric energy in the heater of thermal ink jet printhead. We examined a method for increasing the energy efficiency in terms of printhead design, and we found that it relates with an inertance ratio of the rear fluid pass to the front. We proposed a new side shooter thermal ink jet printhead for improvement of the inertance ratio, and we tried to fabricate channels on silicon wafers by a reactive ion etching (RIE). The printhead achieved higher energy efficiency when compared with the conventional design and it has been proved that high energy efficiency enables low consuming energy or high drop energy, and other good characteristics have been also obtained by the printhead.

Journal of Imaging Science and Technology 43: 332–338 (1999)

Introduction

Since personal computers have been spread widely and Internet environments have been prepared rapidly, people can get various fine images that they want from all over the world. In addition, because digital cameras have become cheaper and the pixel number of CCD has increased (already exceeding 'Mega-Pixel'), we can see high quality images on our computers at home easily. As a natural desire, we want to print these images on paper and see them in our hands.

Recently, most office documents have been colored to appeal to readers. So, the demand for producing many high quality color documents at high speeds has been increased today.

In these situations, small, inexpensive, high image quality, high speed and highly reliable color printers have become more desirable. We believe, and it is recognized in the market, that thermal ink jet (TIJ) printing has a high potential to satisfy these demands in both home and office environments because ink drop ejection and the printing mechanism in thermal ink jet are very simple.

In order to respond to the above market demands, it is important to consider how little energy TIJ printhead consumes and the high performance it offers. Namely, we must consider such a printhead design that can effectively transfer input electric energy to a desired drop performance. We call this transformation efficiency *energy efficiency* of TIJ printhead. If we can get high efficiency, we will be able to achieve low energy consumption

to get a desired performance (drop volume), or get a high performance (drop velocity) at the same consuming energy. The former case makes the printer size smaller and decreases its cost. The latter can widen the variety of inks and decrease maintenance work load, and consequently achieve high image quality and high reliability.

Energy Loss in Thermal Ink Jet and Definition of Energy Efficiency

Figure 1 shows the schematic diagram of a typical side shooter TIJ printhead. After an electric pulse of several microseconds is applied to the heater, the temperature on the heater surface increases rapidly and reaches to a superheat temperature. Homogeneous nucleation occurs, and a vapor bubble is generated with high pressure. The high pressure bubble pushes ink both forward (to the nozzle) and backward (to the reservoir). The pushed ink overcomes surface tension of the meniscus and forms an ink drop.

In this process, when electric energy supplied from the power source is changed to ink drop energy, a great amount of energy loss occurs. The energy losses can be classified by physical phenomena or locations where they occur:

1. Electric loss in electrode and driver (IR drop): electric energy changes only partially into heat due to the resistance of electrode and driver.
2. Thermal transfer around the heater: heat generated at the heater layer is transferred not only to the upper, but also to the lower and side directions.
3. Bubble generation: not all of the energy transferred to the interface of heater surface and ink contributes to bubble generations and growth.

Original manuscript received July 10, 1998

▲ IS&T Member

©1999, IS&T—The Society for Imaging Science and Technology

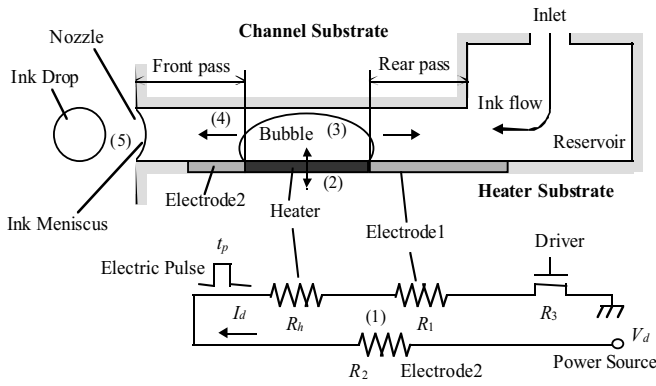


Figure 1. Schematic diagram of a typical side shooter TIJ printhead. The number designates the order in which phenomena occur or the locations where energy losses occur in the drop ejection process.

4. Pressure propagation (distribution) in the fluid pass: bubble pressure pushes ink both to the nozzle and to the reservoir.
5. Surface tension at the nozzle: surface tension resists ink movement and drop formation.

In the above classification, the 4th term, pressure propagation (distribution), depends on the fluid pass design. IR drop and thermal transfer are of course important subjects in printhead design, but they will be argued on another occasion. Herein, we discuss the improvement of pressure propagation by modification of fluid pass design.

Transducer effectiveness as a relation of ejected drop volume and transducer displacement was investigated and the effectiveness was compared between Piezo and TIJ printheads.¹

First, we define energy efficiency (EF) in thermal ink jet printhead as a ratio of drop energy E_d to consuming energy consumed by the heater E_h .²

$$EF = \frac{E_d}{E_h} \quad (1)$$

Energy consumed by the heater E_h is estimated as

$$E_h = I_d^2 \cdot R_h \cdot t_p \quad (2)$$

where I_d , R_h and t_p are electric current, heater resistance and pulse width, respectively. Defining this energy as Eq. 2 can exclude the effect of IR drop in the electrode and driver in this discussion. Drop energy is the sum of drop kinetic energy E_k and surface energy E_s given by³

$$E_k = \frac{1}{2} \cdot m_d \cdot v_d^2 \quad (3)$$

$$E_s = 4 \cdot \pi \cdot r_d^2 \cdot \sigma \quad (4)$$

where m_d , v_d , r_d are the mass of ejected ink drop, initial velocity, and drop radius respectively and σ is an ink surface tension. Drop radius r_d is calculated as the radius of a complete sphere based on the measured mass, including satellite drops.

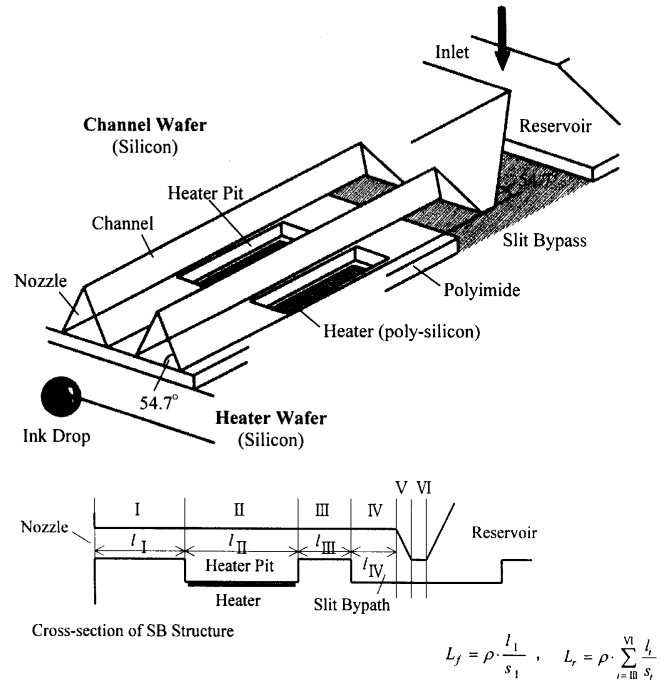


Figure 2. Fuji Xerox conventional TIJ printhead (Slit Bypass [SB] design). Printhead has channels fabricated by ODE, heater pit and slit bypass characteristically. Nozzle shape is an isosceles triangle with 54.7° base angle. (Roman numerals indicate divided pass for calculation of inertance.)

Comparison of Energy Efficiency and Inertance Ratio in Various TIJ Printheads

Considering the ink motion by bubble growth in the fluid pass, we examined the relationship of ink mobility (namely, the reverse of pressure loss) with fluid pass structure. Pressure loss Δp is described as⁴

$$\Delta p = L \cdot \frac{dq}{dt} + R \cdot q \quad (5)$$

where L and R are inertance and resistance respectively, and q is the flow rate of ink. As we can see from this equation, in a rapid motion like a bubble growth ($\leq 10 \mu s$), the inertance is dominant in ink mobility.

We considered that the ratio of heater rear inertance L_r to heater front inertance L_f relates to the efficiency of bubble pressure propagation toward the nozzle. We defined the inertance ratio K as follows,

$$K = \frac{L_r}{L_f + L_r} \quad (6)$$

Suffixes f and r mean the front and rear pass (refer to Fig. 1). We calculated the inertance of each pass as

$$L = \rho \cdot \sum \frac{l_i}{s_i} \quad (7)$$

where ρ is ink density, l and s are fluid pass length and cross-sectional area.

Figure 2 shows the schematic diagram of our conventional side shooter thermal ink jet printhead called as Slit Bypass (SB) design.⁵ Channel (fluid pass) is formed by ODE (Orientation Dependent Etching) on a silicon

channel wafer (C/W), hence the cross sectional shape of the channel is an isosceles triangle with 54.7° base angle, and it is difficult to change the width in the middle of channel. Reservoir and inlet are also formed by ODE. A polyimide pattern on the silicon heater wafer (H/W) forms the heater pit and slit bypass. The heater pit prevents air ingestion from the nozzle⁶ and the slit bypass introduces ink from the reservoir to the channel. The heater is located on the pit bottom. Poly-silicon with reduced resistivity by doping is used for the heater to heat ink. High doped polysilicon exists between the heater and Aluminum electrode. Tantalum covers over the heater polysilicon to prevent mechanical damages due to bubble cavitations. (not shown in Fig. 2).

We analyzed our conventional and competitive TIJ printheads (available in the market) having various designs and different nozzle pitches (resolutions), and we calculated their inertance ratio K according to Eqs. 6 and 7. In the calculation of inertance for our SB design, we divided fluid pass into six sections symbolized by roman numerals in Fig. 2, and calculated L_f and L_r by adding each sections' inertance. In the case of cross sectional area changes in a section, e.g., section V, average area is used for Eq. 7. As for the roof shooter design, it is difficult to divide the fluid pass into the front or rear part. We defined that the area above the heater is the front part and the area from the heater to the reservoir is the rear part.

We also evaluated drop volume and drop velocity performances with our dye-based ink and calculated the energy efficiency under standard drive conditions (voltage and pulse width).

Figure 3 shows the relationship of inertance ratio K with energy efficiency between Fuji Xerox and competitive TIJ printheads. When we compare them in terms of the energy efficiency, it is necessary to note that the energy loss in the thermal transfer process depends on heater layer structure. We neglected it here.

The physical properties of dye-based ink used in evaluations are also shown in Fig. 3.

Inertance ratio K has a good correlation with energy efficiency among various designs of printheads. In the experiments, Roof Shooter B showed high efficiency because of high inertance ratio. As usual, the roof shooter is obliged to have a 2D alignment of heaters and nozzles, and the space from heater to nozzle can become large. Therefore the roof shooter can have a high inertance ratio. Thus, the printhead size becomes larger in a roof shooter.

Latency in Ink Jet Printers

High drop in kinetic energy is necessary to keep high reliability in ink jet printers for the following reason. When drop ejection is halted, ink viscosity near the nozzle becomes higher because of evaporation of ink components with low boiling point.⁷ Therefore, the first ejected drop after idling may be misdirected or decelerated by viscous or solidified ink.

Figure 4 shows how the transit time depends on the idle time. Transit time is the time required for an ejected drop to fly from the nozzle to a 1.5 mm distant position, which is measured by an optical drop sensor.⁸ In the worst case (the idle time is too long), no drop is ejected.

We evaluated the image quality insofar as it is affected by the idle time, and defined latency as the idle time generating no image defect. No image defect in our experiment infers that dot displacement from an ideal position is under $30\ \mu\text{m}$ on paper at a 1.5 mm distance from the nozzle.

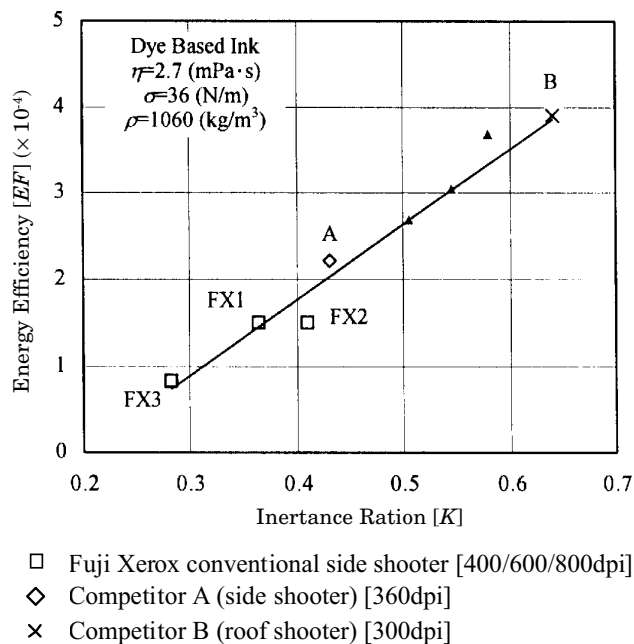


Figure 3. Inertance ratio versus efficiency. Inertance ratio has a high correlation with energy efficiency. (Small triangle symbol designates Trench printhead data, explained later in this paper.)

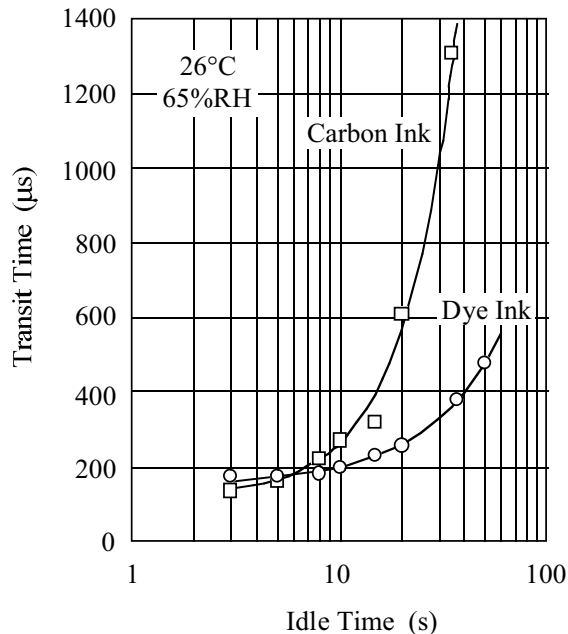


Figure 4. Transit time depends on idle time and ink. Carbon black ink is worse in latency than dye-based ink.

Figure 5 shows photographs of printed dots on paper. In Photo (a), the first dots' displacement is under $30\ \mu\text{m}$ and the image quality is judged as fair; the displacement in Photo (b) is just over $30\ \mu\text{m}$ and defines this idle time as latency.

If we can get a long latency, it is possible to extend the maintenance interval, namely by decreasing the amount of ink consumed by dummy jetting and vacuuming to exhaust viscous ink, thereby enhancing productivity.

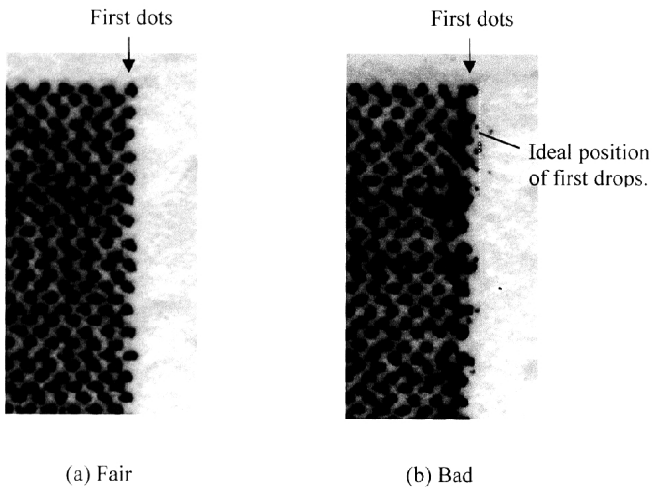


Figure 5. Image defects and latency criteria in terms of dot displacement. First dots in Photo (b) are 30 μm from an ideal position, and the idle time in this case is defined as latency.

According to our experiments, latency also depends on ink components (formulations). Text quality with carbon black ink is superior to that with dye-based ink. Our experiments, however, showed that carbon black ink is worse in latency than dye based ink. We also measured latency and performance with carbon black ink (HP Desk Jet 850C black ink).

Figure 6 shows the relationship between measured latency and drop kinetic energy with 850C black ink (rectangular symbols with solid line). In this experiment, we obtained various kinetic energies by changing the drive conditions (voltage, pulse width) or using different designed printheads. We can see from Fig. 6 that when the drop kinetic energy becomes higher, latency, one of printer reliability, becomes longer. In most cases, drop volume is fixed by image quality (dot size), so high kinetic energy means high velocity. High drop velocity is necessary to obtain a long latency.

New TIJ Printhead with Channels Formed by Silicon Reactive Ion Etching (RIE)

In our conventional design shown in Fig. 2, desired drop volume almost fixes the nozzle width and even the channel width, because the channel is shaped by ODE. If we want to increase the inertance ratio to improve the energy efficiency based on Fig. 3, the length of the rear channel will be long. But in this case, the resistance of the rear channel will be also increased, and it deteriorates the efficiency of the ink refill, which occurs over a relatively long time (100 to 200 μs). To obtain higher drop velocity, the nozzle width is reduced further with larger heater size, and in this case, to keep a high inertance ratio, the rear resistance will be larger and the energy consumed will be increased further because of large heater size.

If we can narrow only the nozzle width that dominates the drop volume and velocity, and expand pass width, we will be able to achieve a high inertance ratio with a low resistance. To realize this design concept, it is important to enlarge the difference between nozzle and channel width.

One of the methods to narrow the nozzle is plastic injection molding compiled with laser ablation. By this method, however, it is difficult to make a large difference in width due to fabrication problems. Another problem is that the

TABLE I. Physical Properties of Typical Materials for Channel Substrate

Material	Thermal Conductivity ($\text{W} \cdot \text{m}^{-1} \cdot \text{K}^{-1}$)	Coefficient of Thermal Expansion ($10^{-5} \cdot \text{K}^{-1}$)
Silicon	168	0.415
Polysulfone	0.15	5.5
Polyethersulfone	0.26	5.5

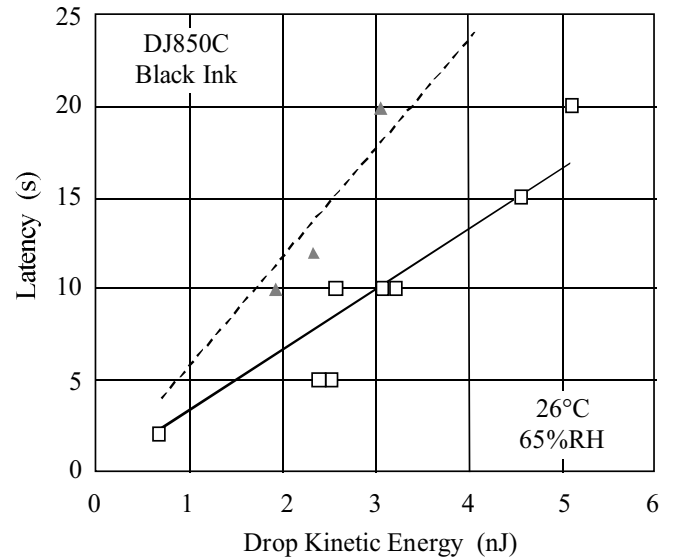


Figure 6. Latency dependence on drop kinetic energy. High kinetic energy can extend Latency. (Triangle symbols with dotted line will be explained later in this paper.)

difference in the thermal expansion coefficients is large between plastic and silicon materials comprising the heater substrate. Thermal conductivity is also low, which affects the thermal accumulation of the printhead.

Table I shows the physical properties (the coefficient of thermal expansion and thermal conductivity) of silicon and typical materials used in this plastic fabrication method. This method is unsuitable to increase the nozzle number with a long printhead due to the gap or stress being large between the channel and the heater substrate.

Considering the above problems, namely, the difference between the nozzle and other pass width, thermal expansion, and thermal conductivity, we focused on silicon reactive ion etching (RIE)⁹ as a channel fabrication method. We tried to fabricate a new printhead using this method to achieve better energy efficiency than our conventional printhead.

Next, we explain the channel fabrication process in this new printhead. Inlet and reservoir are formed by ODE first, in the same manner as our conventional printhead. ODE has a high etching rate in comparison with RIE for silicon, hence it is useful to form a deep hole like a reservoir. Next, channels (fluid pass) are formed by RIE and a rectangular shaped nozzle is formed by dicing an aligned and bonded channel and heater wafer.¹⁰

Figure 7 shows the schematic diagram of a new printhead with channels fabricated by silicon RIE.

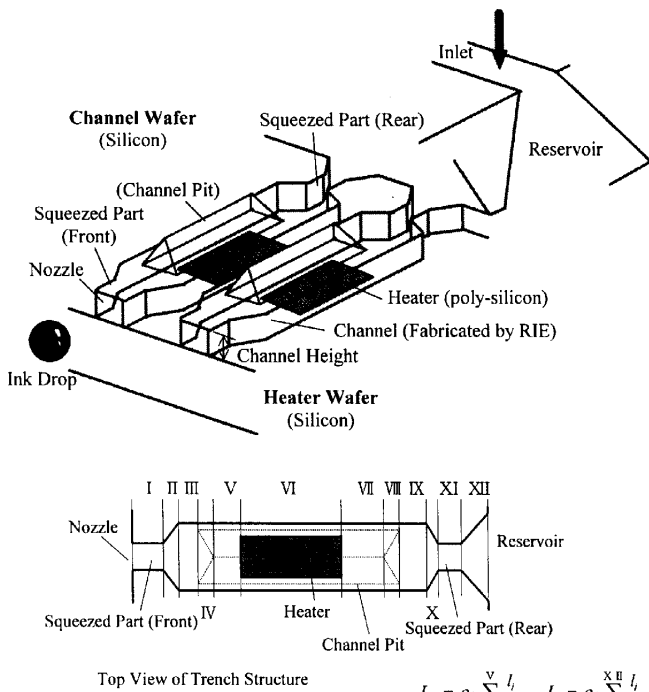


Figure 7. Fuji Xerox new Thermal Ink Jet Printhead (Trench Design). Channels are fabricated by RIE. Channel pit can be obtained by additional ODE process. (Roman numerals in top view means divided pass for calculation of inertia).

Channel height is fixed by etching time and rate, and the etching rate depends on ion acceleration energy. Etching direction in RIE is also anisotropic because of ion rectilinearity. We can obtain an accurate rectangular shape and size of channel over the printhead by controlling the etching time and energy.

We squeezed the channel around the nozzle and at the entrance to the channel from the reservoir. We call this type of printhead the Trench design. In this design, the front squeezed length is important. If the length becomes longer, the front inertia will be larger. However, if it is too short, the meniscus after jetting will become extended and the capillary force will not act sufficiently in the refill process.

If we add one more ODE process, we can obtain a channel pit as shown in Fig. 7. In this design, the channel size is extended, so the resistance of channel will be decreased further.¹¹ Also in the calculation of inertia for the Trench design, we divided fluid pass into twelve parts as shown in Fig. 7. L_f is calculated by addition of each inertia from the part I to V. L_r is from VII to XII.

Figure 8 shows on SEM photograph of the channels formed by RIE from one of the new printhead designs. Nozzle pitch is about 32 μm , which corresponds to 800 dpi. From this photo, it can be realized that channels are formed accurately even at a high resolution of 800 dpi. We believe this method can be applied to over 1600 dpi.

We designed some printheads with nozzle pitches corresponding to 400 dpi and 800 dpi (with and without a channel pit), and we evaluated their performances using our dye-based ink and DJ850C black ink.

Performances of a Newly Designed Printhead

The performance of a new Trench design printhead is given in Table II. The performance of our conventional design (Slit Bypass) is also given in the same table for comparison. In both 400 dpi and 800 dpi/printheads,

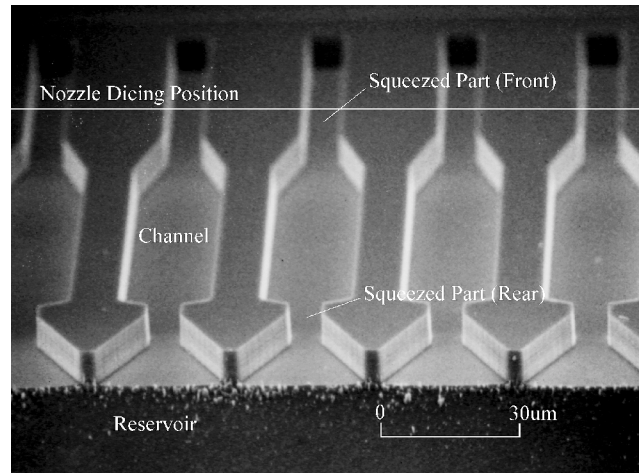


Figure 8. SEM photograph of channels formed by RIE (without channel pit). Channels are aligned in 800 dpi.

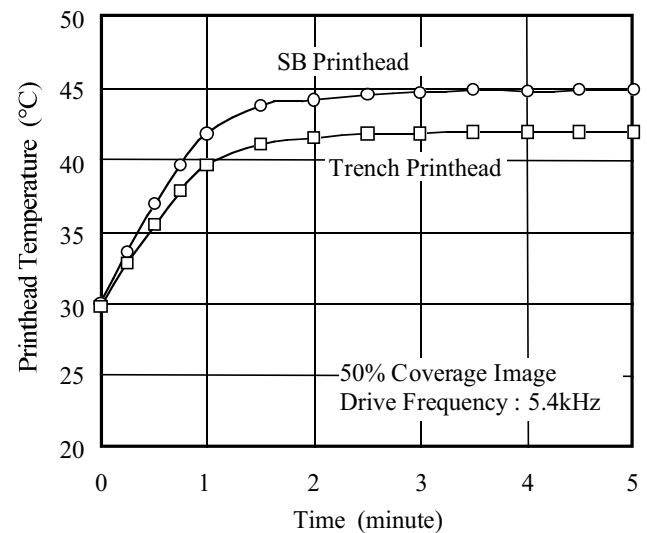


Figure 9. Printhead temperature increase due to printing high coverage images. Both printhead have the same heat sink size.

the energy efficiency of the new design (Trench) was more than 2 times greater, compared with the conventional design.

The relationship between the inertia ratio and energy efficiency in the new Trench printhead also conforms to the trend in Fig. 3. (Small triangle symbols in Fig. 3 mean trench printheads' data.) One of the trench printheads is a match for roof shooter.

In the 400 dpi printhead design, we intended to decrease the consuming energy especially, so the drop energy was increased only 1.4 times than the conventional design, whereas the consuming energy was decreased to 67%. In the 800 dpi design, we aimed to achieve high drop velocity because latency problem becomes more serious at high resolution. As shown in Table II, the kinetic energy with 850C ink increased 2.8 to 3.4 times and latency was extended 5 to 6 times.

High energy efficiency enables low consumption energy or high drop energy depending on the balance of nozzle and heater size in the printhead design.

Figure 9 shows the increase of printhead temperature due to printing of high coverage images. The conventional

TABLE II. Comparison of Performances between New Trench and Conventional SB Design

	Channel Pit	Slit Bypass (Conventional)		Trench (New)		
		-	-	A	A	B
Nozzle Pitch	(dpi)	400	800	400	800	800
Inertance Ratio [K]		0.36	0.28	0.55	0.50	0.57
Heater Energy [E_h]	(μ J)	11.2	5.4	7.5	4.8	4.5
Drop Volume [m_d]	(ng)	37.8	10.6	43.4	14.0	12.3
Drop Velocity [v_d]	(m/s)	8.9	8.4	9.8	13.0	16.0
Drop Kinetic Energy [E_d]	(nJ)	1.50	0.37	2.08	1.18	1.57
Surface Energy [E_s]	(nJ)	0.19	0.08	0.21	0.10	0.09
Energy Efficiency [EF]	($\times 10^{-4}$)	1.51	0.84	3.05	2.68	3.70
Drop Volume [m_d]	(ng)	44.2	10.3	50.5	19.1	14.3
Drop Velocity [v_d]	(m/s)	10.8	11.5	11.0	14.2	18.0
Drop Kinetic Energy [E_d]	(nJ)	2.58	0.68	3.05	1.92	2.32
Latency	(s)	10	2	20	10	12

↑ Dye Based Ink
↓ Carbon Ink

Channel Pit A: No Channel Pit
 B: Channel Pit Exists

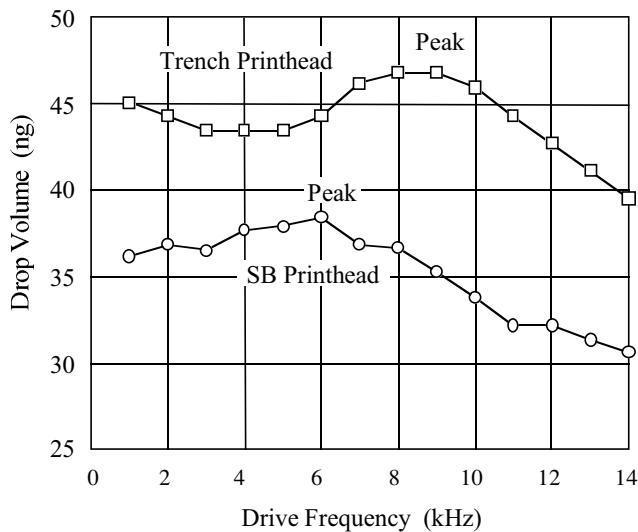


Figure 10. Drop volume dependence on drive frequency. Peak of Trench is 3kHz higher than that of SB.

and new printheads have heat sinks of the same size. Heat accumulation was improved by the Trench printhead.

Latency data of new designed printheads are shown in Fig. 6 again. (Small triangle symbols with dotted line). It appears that a different trend from the conventional exists. We believe that the reason why the Latency of Trench printhead is better than the conventional trend is the effect of the squeezed part near the nozzle for evaporation.

Figure 10 shows the change of drop volume as a function of drive frequency in 400 dpi printheads. Peak of curve corresponds almost to the inverse of the refill time. Peak by the Trench design is about 9kHz—3kHz higher than that by the conventional printhead because of low flow resistance. It enables higher printing frequency in printer. The oscillation of the trench volume curve is larger than that of the SB for low resistance as well.

Low flow resistance is good not only for refill speed but also bubble management in the reservoir and ink

tube. Temperature increase due to printing generates bubbles from ink and enlarges their size. Enlarged bubbles prevent ink flow, so vacuuming is necessary periodically. Mobility of a bubble under vacuuming depends on its size and ink flow velocity, namely flow rate. According to Eq. 8, under the constant vacuum pressure P_V , steady flow rate Q becomes larger as the total resistance of ink pass R_T becomes smaller.

$$Q = \frac{P_V}{R_T} \tag{8}$$

We can reduce R_T by adopting the Trench printhead with small channel resistance R_{ch} , because R_T is described as

$$R_T = \frac{R_{ch} \cdot R_D}{N_{ch} \cdot R_D + N_D \cdot R_{ch}} + R_r + R_{pipe} \tag{9}$$

where R_{ch} , R_d , R_r and R_{pipe} are the resistance of channel, dummy channel not being used for printing, reservoir and pipe from the ink tank to the printhead. N_{ch} and N_d are the number of channels and dummy channels.

Figure 11 shows the distribution of calculated flow velocity in printheads for SB and Trench design with 400 dpi nozzle pitch. In this figure, the flow velocity is slower as color gets darker. It is clear that the dead water area (low velocity area) in the trench printhead is smaller than the SB printhead. We expect that the interval of vacuuming will be longer due to an increase in time for bubble growth to close channels.

Conclusion

We found that improvement of inertance ratio of the rear to the front is effective to increase the energy efficiency. Based on this point and other fabrication problems, we proposed a new thermal ink jet printhead with channels fabricated by silicon reactive ion etching. The new printhead showed high energy efficiency as we expected. It has been demonstrated that this high efficiency enables low energy consumption or high drop energy. The new printhead also showed other good characteristics (temperature accumulation, ink refill

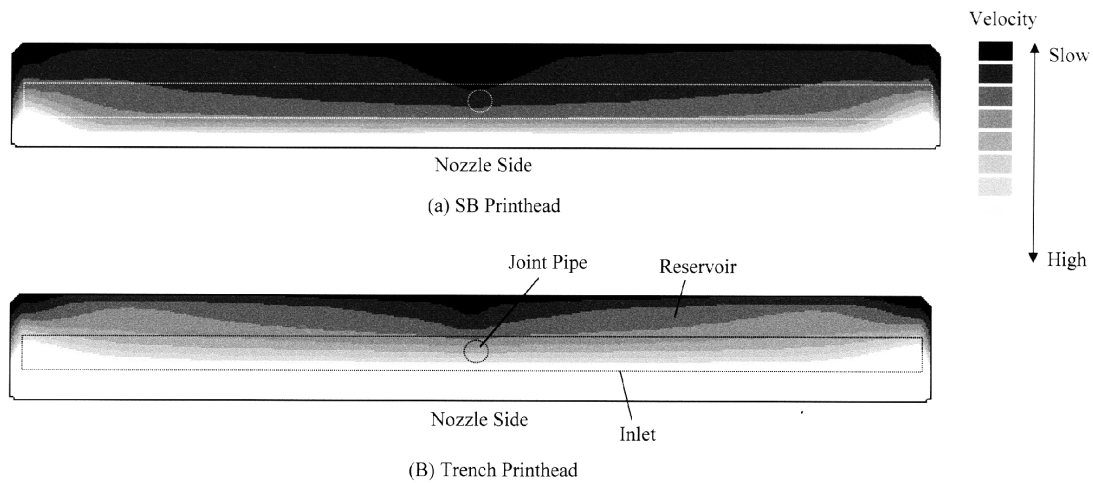



Figure 11. Calculated ink flow velocity distribution in reservoir and channels. Dark tones indicate slow velocity area. Dead water area in Trench is smaller than that in SB. Velocity is high on both sides for dummy channels with reduced resistance.

time and bubble management). The type of printhead that we proposed herein has advantages for high quality and high speed printing which satisfies the market demands. 

Acknowledgment. We would like to thank M. Murata and R. Nayve for suggestions on printhead design from the standpoint of RIE process and channel fabrication. We are also thankful to A. Tohma for assistance with performance evaluations.

References

1. S. F. Pond, Drop-On-Demand Ink Jet Transducer Effectiveness, *IS&T's Tenth International Congress on Advances in Non-Impact Printing Technologies*, IS&T, Springfield, VA, 1994, p. 414.
2. B. Hockwind, Design of Micromechanical Bubble-Jet Devices, *IS&T's 9th International Congress on Advances in Non-Impact Printing Technologies*, 1993, IS&T, Springfield, VA, p. 237.
3. S. Hirata, *IEICE TRANS. ELECTRON E80-C*, 214 (1997).
4. N. Deshapande, *J. Imaging Sci. Technol.* **40**, 396, (1996).
5. M. Fujii, Japan Patent H03-348525 (1991).
6. P. A. Torpey, Prevention of Air Ingestion in a Thermal Ink Jet Device, *IS&T's 4th International Congress on Advances in Non-Impact Printing Technologies*, 1988, IS&T, Springfield, VA, p. 275 .
7. P. A. Torpey, Evaporation of A Two-Component Ink from The Nozzles of A Thermal Ink Jet Printhead, *IS&T's 6th International Congress on Advances in Non-Impact Printing Technologies*, 1990, IS&T, Springfield, VA, p. 453.
8. M. Fujii, Optical Drop Sensor of Continuous Ink Jet Printer, *Proc. of the Nineteenth Joint Conference on Image Technology*, 1988, Tokyo, Japan, p. 83 (In Japanese).
9. J. K. Bhaerdwaj, *SPIE* **2639**, 224 (1995).
10. R. Nayve and M. Fujii, Japan Patent H09-341658 (1997).
11. M. Murata and M. Fujii, Japan Patent H09-341659 (1997).